Archives of Hydro-Engineering and Environmental Mechanics
Vol. 43 (1996), No. 1–4, pp. 21–42

Bedload Under Asymmetric and Irregular Waves: Theory Versus Laboratory Data

Leszek M. Kaczmarek, Rafał Ostrowski

Polish Academy of Sciences Institute of Hydro-Engineering, ul. Kościerska 7, 80–953 Gdańsk, Poland

(Received February 20, 1997; revised April 15, 1997)

Abstract

The results of laboratory bedload measurements are presented. The study comprises a wide range of regular-asymmetric and irregular wave conditions in the ripple regime. A new theoretical model of the moveable bed boundary layer is used for computation of sedimentation volume in the sand trap. The theoretical results are tested against experimental data.

1. Introduction

The model is based on the concept proposed by Kaczmarek & O'Connor (1993) who used the procedure for matching the solutions of equation of motion in the turbulent flow above the theoretical bed level and in the collision-dominated granular-fluid region. This concept, first used for regular linear waves, has recently been developed for random waves by Kaczmarek et al. (1994) and for non-linear waves by Kaczmarek (1995).

Then, on the above basis, the first attempt was made by Kaczmarek et al. (1995) to formulate bedload theory and verify it using available laboratory data and IBW PAN radio-tracer field results. The summary of theoretical findings obtained by use of the unbiased bedload model for both regular and irregular waves was presented by Kaczmarek et al. (1996).

This paper mainly concerns the results of experiments carried out at IBW PAN laboratory. The verification of the theory for regular and irregular waves using own experimental data was the major goal of the study. There are few experimental data sets for the ripple regime, especially in the range $\theta_{2.5} = 0.1 \div 0.4$. Therefore the laboratory survey covered this range, particularly taking into account the identification of non-linear effects. This range of small $\theta_{2.5}$ is extremely important as one can expect the equivalence of bedload and total sediment transport in this regime (small suspended load rate). Thus, only in this regime can the bedload theory be precisely verified while in more severe hydrodynamic conditions bedload is a minor part of the total sediment transport.

A concise description of the theoretical model (with some reference to earlier studies) is given in Section 2 of the paper. The details of laboratory survey, comparison of experimental and theoretical data and discussion are presented in Section 3.

2. Theoretical Bedload Model

2.1. Basic Equations

The nearbed dynamics is modelled for the flow regions above and beneath the original static bed line, see Figure 1. The collision-dominated granular-fluid region I stretches below the nominal static bed while the wall-bounded turbulent fluid region II extends above it. Since both water and sand grains are assumed to move in both regions, there must be a certain transition zone between I and II, in which the velocity and stress profiles of I and II would merge and preserve continuity of shape. The intersection of the two velocity profiles is marked as point A in Figure 1.

The flow in the turbulent upper region for **regular** waves is described by the integral momentum model based on the solution proposed by Fredsœ (1984), developed and adapted – *inter alia* – for non-linear waves by Kaczmarek & Ostrowski (1992).

The approach for **irregular** waves incorporates a time-invariant, two-layer eddy viscosity model including the representative parameters: friction velocity and bottom boundary layer thickness. Bed roughness is calculated using the method proposed by Kaczmarek (1995), taking into account the reduction of this parameter due to irregularity of wave motion. More detailed discussion on modelling of bed roughness is given in section 2.2

The problem for **irregular** waves is closed by the iterative scheme for finding the wave period representing the random wave field (T_r) – see Scheme 1. The scheme allows to solve the task associated with the appropriate choice of the equivalent wave period and to include the coupling effects between the harmonic components, incorporated in the eddy viscosity. The detailed description of the above can be found in Kaczmarek & Ostrowski (1995).

In the sub-bed flow region, the sediment concentration is high and chaotic collisions of grains are the predominant mechanism. Particle interactions are assumed to produce two distinct types of behaviour. The Coulomb friction between particles give rise to rate-independent stresses (of the plastic type) and the particle collisions bring about stresses that are rate-dependent (of the viscous type). The use of the mathematical description by Sayed & Savage (1983) for determination of the stress tensor was made and the balance of linear momentum according to Kaczmarek & O'Connor (1993) leads to the following equations:

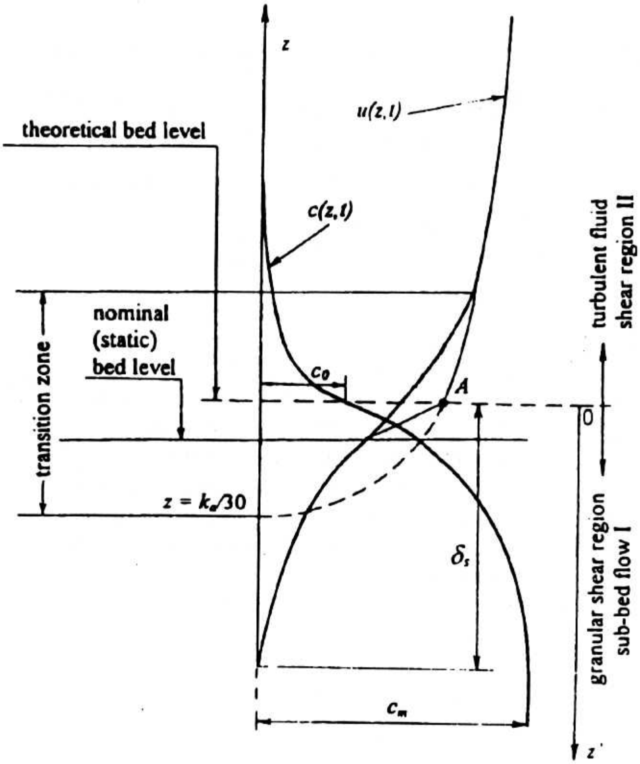

Fig. 1. Definition sketch

$$\alpha^0 \left[\frac{c - c_0}{c_m - c}\right] \sin\varphi \sin 2\psi + \mu_1 \left[\frac{\partial u}{\partial z'}\right]^2 = \rho u_f^2 \tag{1}$$

$$\alpha^0 \left[\frac{c - c_0}{c_m - c}\right] (1 - \sin\varphi \cos 2\psi) + (\mu_0 + \mu_2) \left[\frac{\partial u}{\partial z'}\right]^2 =$$

$$= \left[\frac{\mu_0 + \mu_2}{\mu_1}\right]_{c=c_0} \rho u_f^2 + (\rho_s - \rho) g \int_0^{z'} c\,dz \tag{2}$$

in which:

ρ_s and ρ are the densities of the solid and fluid, respectively,

α^0 is a constant,

c_0 and c_m are the solid concentrations corresponding to fluidity and the closest packing, respectively,

μ_0, μ_1 and μ_2 are functions of the solid concentration c:

$$\frac{\mu_1}{\rho_s d^2} = \frac{0.03}{(c_m - c)^{1.5}}, \tag{3}$$

Scheme 1. Computation of bedload under irregular waves

< 1 >	Fourier decomposition of the free stream velocity input $U(t)$ $$U(t) = \sum_n U_n \sin(n\omega t + \varphi_n) + \tfrac{1}{2}U_0$$
< 1a >	*Alternatively* Fourier decomposition of the water surface elevation input $\eta(t)$ $$U(t) = \sum_n \eta_n \frac{n\omega}{\sinh(k_n h)} \sin(n\omega t + \varphi_n) + \tfrac{1}{2}U_0$$
< 2 >	Calculation of the input root mean square value: $$U_{rms} = \sqrt{\sum_n U_n^2}$$
< 3 >	Computation of bed roughness for irregular waves
< 4 >	Assumption of representative period T_r
< 5 >	Determination of parameters of representative eddy viscosity distribution: u_{fr} & δ_r (running Fredsœ's (1984) model with U_{rms} & T_r as an input)
< 6 >	Computation of representative shear stress amplitude ρu_{fB}^2 (using Brevik's (1981) approach with U_{rms}, T_r & eddy viscosity distribution from step < 5 > as an input)
< 7 >	Computation of bed shear stress components τ_n & $\varphi_{\tau n}$ using Brevik's approach with U_n, $n\omega$ (from step < 1 > or < 1a >) and representative eddy viscosity (determined in step < 5 >) as an input
< 8 >	Calculation of bed shear stress root mean square value: $$\tau_{rms} = \sqrt{\sum_n \tau_n^2}$$
< 9 >	Checking whether ρu_{fB}^2 (step < 6 >) $= \tau_{rms}$ (step < 7 >) if NO $\longrightarrow$ correction of T_r and going to step < 5 > if YES $\longrightarrow$ going to step < 10 >
< 10 >	Calculation of output time series (bed shear stress): $$\rho u_f^2(t) = \tau(t) = \sum_n \tau_n \sin(n\omega t + \varphi_n + \varphi_{\tau n})$$
< 11 >	Calculation of bedload time series with the boundary conditions $u_f\|_{z'=0} = u_f(t)$ using model presented in section 2.3

$$\frac{\mu_0 + \mu_2}{\rho_s d^2} = \frac{0.02}{(c_m - c)^{1.75}}. \tag{4}$$

The value φ in Equations (1) i (2) is the quasi-static angle of internal friction, while the quantity ψ is equal to:

$$\psi = \frac{\pi}{4} - \frac{\varphi}{2}. \tag{5}$$

For the calculations the following numerical values are recommended:

$$\frac{\alpha^0}{\rho_s g d} = 1 \quad c_0 = 0.32 \quad c_m = 0.53 \quad \varphi = 24.4^\circ.$$

where d denotes the diameter of grains.

2.2. Moveable Bed Roughness

The apparent bed roughness parameter k_a is a central quantity in the model. Both the turbulent and sub-bed velocity profiles depend on k_a, which is not known a priori. Therefore an iteration procedure is proposed for finding the matching point A between these profiles. The matching is assumed to take place at the phase of maximum shear stress, although at any other phase of oscillatory motion there must be some transition between the two profiles. The new theoretical approach for the evaluation of moveable bed roughness under regular and irregular waves, sinusoidal/asymmetric waves with/versus currents has been proposed by Kaczmarek (1995). Here, the advantage is taken of solutions obtained for the cases of regular and irregular waves without currents.

For engineering purposes it is useful to approximate the theoretical results by a curve expressed in terms of skin friction. To determine the skin friction one can follow Nielsen's (1992) description:

$$\theta_{2.5} = \frac{0.5 f_{2.5}(a_{1m}\omega)^2}{(s-1)gd}, \tag{6}$$

$$f_{2.5} = \exp\left[5.213\left(\frac{2.5d}{a_{1m}}\right)^{0.194} - 5.977\right] \tag{7}$$

in which $s = \rho_s/\rho$.

The parameter $\theta_{2.5}$ is introduced for the sake of approximation of theoretical bed roughness and bedload results as well as presentation of experimental data.

The ability of the new theoretical approach to predict the moveable bed roughness height has been demonstrated and confirmed in various contexts by Kaczmarek (1995), Kaczmarek et al. (1995) and Kaczmarek et al. (1996) using a wide range of available laboratory and field data. The results of theoretical modelling have shown quite the opposite trend of behaviour of the roughness parameter to those suggested by many authors, where the roughness parameter increases drastically with increasing transport intensity. It has been shown that the roughness parameter decreases with increasing dimensionless maximum shear stress (Shields parameter). This finding, however, can be verified directly only by a few experimental data sets presented by Nielsen (1992) while it is consistent indirectly – via bedload quantities, friction factors etc. – with the bulk of other laboratory and field results.

The model was run for a wide range of small and large scale conditions and for a few diameters of sandy bed. Then the results were approximated yielding the following formulae for **regular** and **irregular** waves, respectively:

$$\frac{k_a}{d} = 47.03\theta_{2.5}^{-0.66} \tag{8}$$

$$\frac{k_a}{d} = 26.64\theta_{2.5}^{-0.71} \tag{9}$$

For **irregular** waves k_a is calculated using Equation (9) taking root-mean-square wave height (or free stream velocity) and peak period for determination of $\theta_{2.5}$. Then bedload rate series is modelled following steps $< 4 >$–$< 11 >$ of the computational procedure shown in Scheme 1.

2.3. Bedload Transport

Once k_a is determined the velocity distributions can be computed for regions I and II, as well as the concentration of grains in the bedload layer.

Basing on Bagnold's definition, according to which the bedload is a part of sediment transport subject to inter-granular forces, the bedload layer can be represented as region II. Knowing the instantaneous shear stress one can calculate the instantaneous bedload rate from velocity and concentration profiles in this layer:

$$Q_B = \int_0^{\delta_s} u(z', t)c(z', t)\mathrm{d}z \tag{10}$$

The dimensionless bedload rate Φ_B is defined as:

$$\Phi_B = \frac{Q_B}{d\sqrt{(s-1)gd}} \tag{11}$$

It has been found that for **regular** waves the present theoretical results are close to that of Meyer-Peter and their approximation yields the same exponent of 1.5, i.e.:

$$\Phi_{B\max} = 3.4\theta_{2.5}^{1.5} \tag{12}$$

while the approximation of the theoretical results averaged over half wave period $T/2$ reads:

$$\Phi_{T/2} = 1.3\theta_{2.5}^{1.5} \tag{13}$$

3. Laboratory Survey

3.1. Experimental Setup and Procedure

The measurements were carried out in the IBW PAN wave flume. 0.5 m wide and 22.5 m long, this is equipped with a programmable wave maker and can be filled with water up to 0.7 m. Reinforced concrete slabs 8 cm thick were placed on the bottom and the sandy measuring section (also 8 cm thick) 7 m long was situated about the middle of the flume. Natural sand was used in the experiments, with the grain diameter $d_{50} = 0.22$ mm.

For each test, free surface elevation was registered at three points along the flume. The horizontal component of free stream velocity was measured at one point of the measuring section, using a micro-propeller. The micro-propeller and one of the wave gauges were located above the sand trap. The other two wave gauges were spaced $1/4 * L$ from each other (L being a wave length) to estimate the reflection effects in the flume. Experimental setup, together with sand trap, is shown in Figure 2.

The sand trap was covered by a lid and buried in the sandy section before each test. Then the waves were generated until bed ripples were fully formed, which took 25–60 minutes. The lid, suspended on four strings, was removed thereafter, together with a thin layer of sand on it. Then the wave series was continued for 1.2–15 minutes and sediment grains were being accumulated in the sand trap. Finally, the grains were siphoned from the trap and weighed with water in a measuring cylinder. Thus, the amount of sediment could be determined using the formula:

$$V = \frac{\Delta m}{\rho_s - \rho} \tag{14}$$

in which Δm is the difference between mass of the cylinder with water + soil and mass of the cylinder with water only.

The sand trap had two cells to ensure the determination of onshore and offshore bedload components. The sum of these components has been assumed to represent the dimensionless bedload rate $\Phi_{T/2}$, cumulated during the time of the test.

Together with the sedimentation, bed form geometry was measured and shape assessed after each test.

3.2. Experimental Parameters and Results

During each test a constant water depth of $h = 0.5$ m was maintained above the measuring section. The measurements were carried out for six sets of parameters for regular waves (Tests 1, 2, 3, 4, 11 and 12) and six irregular wave series (Tests 5, 7, 8 for JONSWAP and Tests 6, 9, 10 for Pierson-Moskowitz spectrum generated by the wave maker). The experiments comprised a few tests for each set of wave parameters. In all, 141 series were run, among which 103 were regular.

The results for **regular**-asymmetric waves in comparison with theoretical bedload data, together with wave parameters, are shown in Figure 3. The conformity of theoretical evaluations and experimental data can be seen, especially while using the non-linear approach (except for Test 2). It should be pointed out that for long

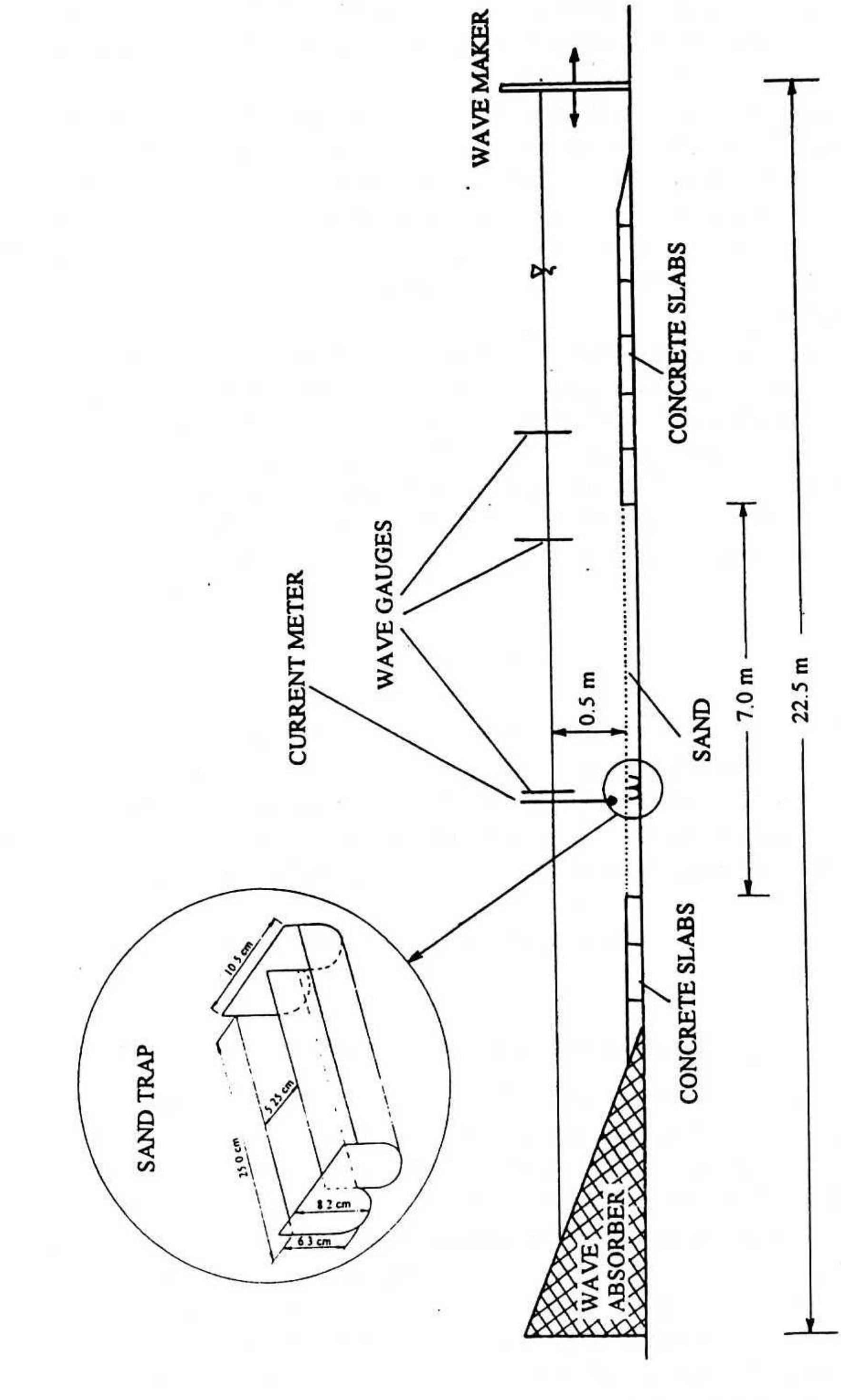

Fig. 2. Experimental setup

and highly asymmetric waves, represented by Test 11 (Ursell parameter amounts to 40), the experimental data fit the present non-linear theory while they differ significantly from the linear approach. The most severe shear stress conditions without wave breaking, attaining $\theta_{2.5} = 0.4$, were achieved in Test 12, however, the Ursell parameter (equalled to 31) was less than in Test 11. In test 12 a very distinct concentration of suspended sediment was observed which could result in increased accumulation in the sand trap, bigger than theoretically modelled, using both linear and non-linear theory.

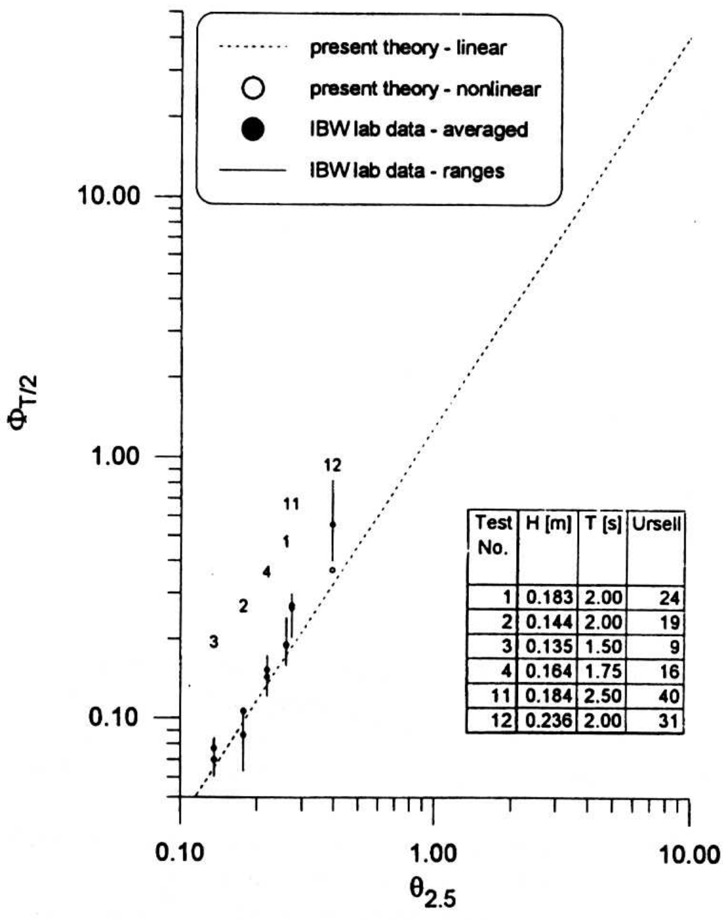

Test No.	H [m]	T [s]	Ursell
1	0.183	2.00	24
2	0.144	2.00	19
3	0.135	1.50	9
4	0.164	1.75	16
11	0.184	2.50	40
12	0.236	2.00	31

Fig. 3. Bedload laboratory data vs. present linear and non-linear theory for regular waves

The detailed results for regular waves, i.e. wave parameters at the wave maker, ripple geometry, reflection coefficients and sedimentation rates, are given in Appendix – Tables 1, 2 and 3. It should be mentioned that for regular waves a few experimental sedimentation values – registered in disturbed conditions, e.g. during occurrence of distinct scours at sand trap edges – have not been included in the plots while they are all given in Tables of Appendix, with appropriate comments.

The laboratory bedload data for **irregular** waves in comparison with theoretical results are depicted in Figure 4. Computed values have been modelled using the present theory, i.e. Equations (1)–(7), (9)–(11), and Scheme 1, on the basis of full-time (15 minutes) water surface elevation series registered at the measuring section. Conformity between theoretical and experimental results appears to be very good.

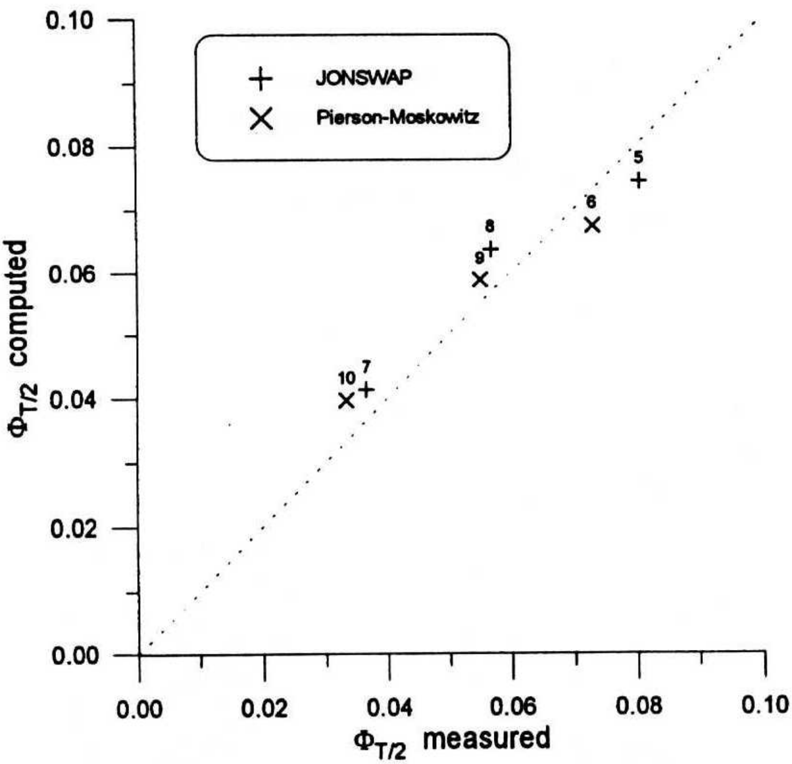

Fig. 4. Bedload laboratory data vs. present theory for irregular waves

The irregular wave parameters at the wave maker, ripple geometry, reflection coefficients and sedimentation rates are given in the Appendix – Table 4, while the parameters computed and registered at the measuring section are presented in Table 5 of the Appendix.

Although net transport effects are not discussed in the present paper, offshore and onshore sediment transport components are distinguished in Tables 1–4 of the Appendix to provide more extensive information on the experimental results.

For the sake of full comparison the laboratory bedload data for regular and irregular waves are plotted together against the linear theory in Figure 5. The results for irregular waves are presented as a function of dimensionless stress $\theta_{2.5}$, calculated using root-mean-square wave height and representative wave period, see Table 5 in the Appendix.

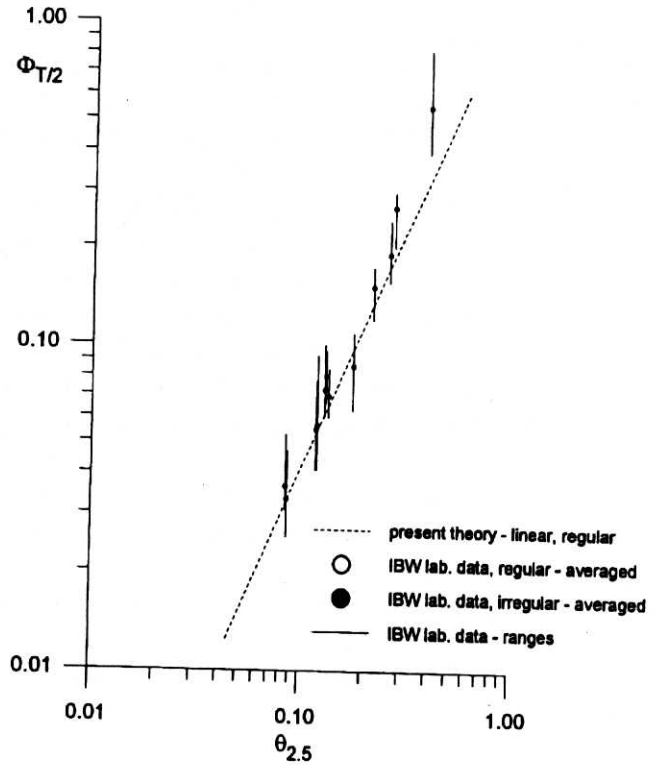

Fig. 5. Bedload laboratory regular and irregular data vs. present linear theory

Figure 5 implies that the bedload rate for irregular cases can be successfully modelled with the use of present linear theory taking root-mean-square wave height H_{rms} and representative wave period T_r as an input. It should be pointed out that computed values of T_r are close to those of T_p, which is depicted in Table 5 of the Appendix. However, further studies are necessary to find out whether this conclusion is valid for other (wider) spectra as well.

It can also be seen from Figure 5 that for weak and moderate shear stress conditions the regular laboratory bedload data lie slightly above the results obtained using the linear theory, thus for precise determination of bedload rate under regular-asymmetric waves a non-linear approach should be used. Finally, it can be concluded that for high shear stresses the present linear theory underestimates bedload rate, most probably due to significant concentration of suspended sediment.

4. Summary and Conclusions

The paper presents the results of comparison between the original bedload theory and experimental data collected by IBW PAN laboratory. The theoretical bedload approach is based on the moveable bed boundary layer concept taking grain-grain interactions into account. The laboratory survey covers the range of ripple regime for relatively small dimensionless Shields parameter. This range is very important as there are few experimental data sets for this regime. Secondly, in this regime one can expect the equivalence of bedload and total sediment transport because the contribution of suspended load is very small.

The compliance between theoretical and experimental results appears to be very good for both regular and irregular waves. It can be concluded that for weak and moderate shear stresses the present linear theory slightly underestimates bedload rate. Hence, for precise determination of bedload rate under regular-asymmetric waves the non-linear approach should be used. For high shear stresses the present linear theory also underestimates bedload rate, however, in this regime, most probably – due to significant contribution of suspended load.

Very good results of comparison between theoretical and experimental data for irregular waves imply the usefulness of the proposed routine of bedload modelling, starting from full-time wave series, calculating reduced roughness, shear stress time series and yielding bedload transport rate series.

It is shown that the bedload rate for irregular waves can be successfully modelled with the use of present linear theory taking root-mean-square wave height and peak period as an input. This conclusion can be important in practical engineering applications.

Acknowledgements

The study was sponsored by KBN and PAN, Poland, under programme 2 IBW PAN, which is hereby gratefully acknowledged. The authors wish to thank Prof. Ryszard B. Zeidler for his support during the project, as the supervisor of the 2 IBW PAN programme. The authors are grateful to Marek Skaja and Marek Szmytkiewicz for helpul suggestions, sharing their experience on laboratory modelling. Our thanks also go to technical staff: Antoni Stojek – for technical supervision of the survey, Tadeusz Perfumowicz – for electronic assistance and Danusia Piotrowska – for edition of graphs.

References

Brevik I. (1981) Oscillatory Rough Turbulent Boundary Layers, *J. Waterway, Port, Coast. and Ocean Engineering, ASCE,* Vol. 107, No. 3, 175–187.

Fredsœ J. (1984), Turbulent boundary layer in wave-current motion, *J. Hydraulic Engineering, ASCE,* Vol. 110, No. 8.

Kaczmarek L. M., Ostrowski R. (1992), Modelling of wave-current boundary layer in the coastal zone, *Proc. 23rd International Conf. Coastal Engineering, ASCE,* New York, 350–363.

Kaczmarek L. M., O'Connor B. A. (1993), *A new theoretical approach for predictive evaluation of wavy roughness on a moveable flat/rippled bed, Parts I/II*, Reports CE/14-15/93, Dept. Civ. Engineering, Univ. Liverpool.

Kaczmarek L. M., Harris J. M., O'Connor B. A. (1994), Modelling moveable bed roughness and friction for spectral waves, *Proc. 24th International Conf. Coastal Engineering, ASCE*, New York, 300–314.

Kaczmarek L. M. (1995), Nonlinear effects of waves and currents on moveable bed roughness and friction, *Arch. of Hydro-Engineering and Environmental Mechanics*, No. 1–2, 3–27.

Kaczmarek L. M., Ostrowski R. (1995), Modelling of bed shear stress under irregular waves, *Arch. of Hydro-Engineering and Environmental Mechanics*, No. 1–2, 29–51.

Kaczmarek L. M., Ostrowski R., Zeidler R. B. (1995), Boundary layer theory and field bedload, *Proc. Intern. Conf. Coast Res.* in *Terms of Large Scale Experiments (Coastal Dynamics '95), ASCE*, 664–675.

Kaczmarek L. M., Ostrowski R., Zeidler R. B. (1996), Unbiased Model for Bedload Due to Waves in Seas and Estuaries, *Hydrotechnical Transactions*, No. 60, 159–176.

Nielsen P. (1992), *Coastal bottom boundary layers and sediment transport*, Advanced Series on Ocean Engineering, Vol. 4, World Scientific, Singapore.

Sayed M., Savage S. B. (1983), Rapid gravity flow of cohesionless granular materials down inclined chutes. *J. Applied Mathematics and Physics (ZAMP)*, Vol. 34, 84–100.

Appendix – Tables

Table 1.

Record of bedload measurements 1996 **Regular waves**

Water depth h=0.5 m

A two-cell sand trap; (+) and (-) denote the *onshore* and *offshore* directed sediment accumulated in the trap, respectively

Table shows wave parameters at the wave maker

Test No.	Date	H [m]	T [s]	Time after which the ripples were measured [min]	Ripple length [mm]	Ripple height [mm]	Ripple shape	Refl. coeff.	Data files	Accum. time [min]	Offshore directed accum. (-) [kg]	Onshore directed accum. (+) [kg]	Remarks
1	12,06	0,20	2,00	60	115	20	regular	0,13	R_02_2	5	0,125	0,185	
					110	20	asymmetric		0106LOG1	5	0,140	0,110	Scour at (+) side
					120	19			0106REF	5,5	0,175	0,230	Sand trap located deeper (as default in next tests)
					115	20				5	0,180	0,215	
					115	19				5	0,115	0,140	Sand trap edges visible
					120	20				5	0,115	0,180	Sand trap edges visible, particularly at (-) side
	19,06	0,20	2,00							5	0,210	0,200	
										5	0,160	0,170	
2	13,06	0,15	2,00	25	100	15	regular	0,13	R_015_2	5	0,020	0,025	Started from flat bed
					90	14	asymmetric		0115LOG1	10	0,050	0,090	
					100	15			0115REF	10	0,063	0,085	
					95	14				10	0,048	0,060	
					95	15				10	0,046	0,055	
										10,5	0,054	0,095	
										10	0,049	0,060	
	17,06	0,15	2,00							10	0,103	0,205	
										10	0,100	0,168	
										10	0,098	0,107	Small scour at (+) side
										10	0,138	0,090	Initially good conditions; later scour at (+) side
	18,06	0,15	2,00							10	0,150	0,200	Initially ripple crest close to (+); later small scour at (-)
										10	0,115	0,200	Visible edge (ripple trough) at (-); ripple crest at (+)
										10	0,100	0,135	Visible edge at (-); very small local scour at (+)

Table 1a continued.

Record of bedload measurements 1996							**Regular waves**						
Water depth h=0.5 m													
A two-cell sand trap; (+) and (-) denote the *onshore* and *offshore* directed sediment accumulated in the trap, respectively													
Table shows wave parameters at the wave maker													
3	14,06	0,15	1,50	30	60	10	regular	0,11	R_015_15	15	0,085	0,130	Started from flat bed
					60	10	asymmetri	0,12	0125LOG1	15	0,120	0,145	Scour at (+) side
					60	8			0125REF	15	0,120	0,105	Scour at (+) side
					60	9			0136LOG1	15	0,065	0,140	Started from flat bed
					70	10			0136REF	15	0,075	0,145	Started from flat bed at (+) side
					60	8							
					65	8							
	17,06	0,15	1,50							10	0,173	0,135	Big ripple crest at (-) side
										10	0,095	0,105	Flatter at (+) side
	18,06	0,15	1,50							10	0,135	0,140	Initially ripple crest effect at (-) side
										10	0,110	0,130	Symmetric bed shape at (+) & (-) sides
										10	0,125	0,105	Symmetric bed shape at (+) & (-) sides
										10	0,090	0,105	Very good initial conditions
4	19,06	0,20	1,75	30	90	14	regular	0,10	R_02_175	10	0,370	0,475	
					100	15	asymmetric		0163LOG1	10	0,305	0,365	
					100	16			0163REF	10	0,235	0,330	
					110	18				10	0,205	0,275	Scours at both sides
					85	17				10	0,190	0,275	Edges visible
					95	15				10	0,225	0,320	After 0.5 hour sand trap covered
					100	16				10			

Table 2.

Record of bedload measurements 1996							**Regular waves**		***Additional tests (new conditions)***				
Water depth h=0.5 m													
A two-cell sand trap; (+) and (-) denote the *onshore* and *offshore* directed sediment accumulated in the trap, respectively													
Table shows wave parameters at the wave maker													
Test No.	Date	H [m]	T [s]	Time after which the ripples were measured [min]	Ripple length [mm]	Ripple height [mm]	Ripple shape	Refl. coeff.	Data files	Accum. time [min]	Offshore directed accum. (-) [kg]	Onshore directed accum. (+) [kg]	Remarks
11	9,07	0,20	2,50	30	140	26	irregular	0,20	R_02_25	4	0,178	0,212	
					135	22	asymmetric		0282LOG1	4	0,149	0,235	
					145	24	moving on-		0282REF	4	0,160	0,204	
					140	26	shore (1 cyc./			4	0,131	0,131	Scour at (+)
					140	21	8-10 min.)			4	0,110	0,101	Scours at (+) & (-)
	15,07	0,20	2,50							4	0,202	0,480	Distinct crest effects at (-) & (+)
										4	0,182	0,282	Crest effect at (+)
										4	0,161	0,191	
										4	0,142	0,302	Crest effect at (+)
										4	0,112	0,205	Visible edge at (-)
										4	0,102	0,221	Small scour at (-)
										4	0,134	0,215	
										4	0,123	0,200	
										4	0,132	0,253	
										4	0,116	0,172	Scour at (+)

Table 2a continued.

Record of bedload measurements 1996							**Regular waves**		***Additional tests (new conditions)***							
Water depth h=0.5 m																
A two-cell sand trap; (+) and (-) denote the *onshore* and *offshore* directed sediment accumulated in the trap, respectively																
Table shows wave parameters at the wave maker																
12	10,07	0,25	2,00	30	120	18	irregular	0,13	R_025_2	3			Immediate scours			
					120	17	asymmetric		0290LOG1							
					125	19	locally 3-D		0290REF							
					120	17										
	11,07	0,25	2,00	thicker layer of sand at the trap						2	0,239	0,299				
										2	0,252	0,222	Lack of sand visible			
										2	0,205	0,165	Small scours at (-) & (+)			
	12,07	0,25	2,00	thicker layer of sand at the trap						1,2	0,155	0,150	Crest effects possible			
										1,2	0,135	0,142				
										1,2	0,123	0,137				
										1,2	0,120	0,127				
										1,2	0,118	0,103				
										1,2	0,110	0,098				
										1,2	0,100	0,087				
										1,2	0,114	0,099				
										1,2	0,120	0,110				
										1,2	0,100	0,085				
										1,2	0,090	0,078	Visible edge at (-)			
										1,2	0,088	0,087	Flat bed at (-) & (+); edges rather invisible			
										1,2	0,080	0,094				
										1,2	0,070	0,085	Small troughs at (-) & (+)			

Table 3.

Record of bedload measurements 1996 | **Regular waves** | ***Repeated tests***

Water depth h=0.5 m

A two-cell sand trap; (+) and (-) denote the *onshore* and *offshore* directed sediment accumulated in the trap, respectively

Table shows wave parameters at the wave maker

Test No.	Date	H [m]	T [s]	Time after which the ripples were measured [min]	Ripple length [mm]	Ripple height [mm]	Ripple shape	Refl. coeff.	Data files	Accum. time [min]	Offshore directed accum. (-) [kg]	Onshore directed accum. (+) [kg]	Remarks
1		0,20	2,00	30	120	18	regular	0,13	R_02_2	5	0,280	0,330	
					120	19	asymmetric		0106LOG1	5	0,195	0,240	
					120	19			0106REF	5	0,155	0,160	Small scour at (+)
					110	18				5	0,125	0,155	Small scour at (+)
					115	18				5	0,130	0,135	Small scour at (+)
					120	20				5	0,120	0,100	Small scour at (+)
					115	19				5	0,135	0,160	Small scour at (+)
					115	19				5	0,075	0,135	Small scour at (+)
2		0,15	2,00	30	95	16	regular	0,13	R_015_2	10	0,165	0,190	
					105	15	asymmetric		0115LOG1	10	0,115	0,160	Small scour at (-); trap edge invisible
					90	16			0115REF	10	0,090	0,130	Small scour at (-); trap edge invisible
					100	14				10	0,090	0,090	
					90	14				10	0,085	0,100	Scours at both sides; trap edges invisible
					100	16				10	0,090	0,090	Scours at both sides; trap edges invisible
					100	16				10	0,065	0,075	Scours at both sides; trap edges invisible
					90	14				10	0,080	0,065	

Table 3a continued.

Record of bedload measurements 1996 — Regular waves — *Repeated tests*

Water depth h=0.5 m

A two-cell sand trap; (+) and (-) denote the *onshore* and *offshore* directed sediment accumulated in the trap, respectively

Table shows wave parameters at the wave maker

Test No.	Date	H [m]	T [s]	Time after which the ripples were measured [min]	Ripple length [mm]	Ripple height [mm]	Ripple shape	Refl. coeff.	Data files	Accum. time [min]	Offshore directed accum. (-) [kg]	Onshore directed accum. (+) [kg]	Remarks
3		0,15	1,50	30	70	10	regular	0,11	R_015_15	10	0,182	0,112	
					65	10		0,12	0125LOG1	10	0,116	0,120	
					70	8	slightly		0125REF	10	0,106	0,110	
					70	12	asymmetric		0136LOG1	10	0,100	0,084	
					65	10	(moving		0136REF	10	0,093	0,087	
					65	9	onshore			10	0,080	0,075	Wide & shallow scour at (+)
					60	10	1 cycle/			10	0,068	0,063	Wide & shallow scour at (+)
					65	8	30 min.)			10	0,075	0,067	Wide & shallow scour at (+)
4	28,06	0,20	1,75	30	105	16	regular	0,10	R_02_175	5	0,232	0,273	
					105	16	asymmetri c		0163LOG1	5	0,162	0,163	
					95	16			0163REF	5	0,115	0,155	
					95	16				5	0,105	0,150	
					90	15				5	0,095	0,165	
										5	0,095	0,170	
										5	0,090	0,110	
										5	0,100	0,095	

Table 4.

Record of bedload measurements 1996 — Irregular waves: JONSWAP (J) & Pierson-Moskowitz (P-M) spectra

Water depth h=0.5 m

A two-cell sand trap; (+) and (-) denote the *onshore* and *offshore* directed sediment accumulated in the trap, respectively

Table shows significant wave height and peak period at the wave maker

Test No.	Date	H [m]	T [s]	Time after which the ripples were measured [min]	Ripple length [mm]	Ripple height [mm]	Ripple shape	Refl. coeff.	Data files	Accum. time [min]	Offshore directed accum. (-) [kg]	Onshore directed accum. (+) [kg]	Remarks
5	20,06	0,20	2,00	60	115	19	regular	0,16	I_02_2	15	0,250	0,220	Ripple crest effects at (-) side
(J)					95	15	symmetric		0177LOG1	15	0,240	0,185	Ripple crest effects at (-) side; small scour at (+) side
					105	17			0177REF	15	0,230	0,185	Ripple crest effects at (-) side; very small scour at (+) side
					95	15				15	0,200	0,170	Very small slope at (-) side; vanishing ripple crest; flatter at (+) side
					110	17				15	0,175	0,150	
					110	17				15	0,175	0,175	
					110	18							
					110	19							
					115	19							
					120	20							
6	21,06	0,20	2,00	60	100	14	regular	0,17	I1_02_2	15	0,260	0,230	Symmetric shape of bed at both (-) & (+) sides
(P-M)					100	15	symmetric		0187LOG1	15	0,205	0,170	Ripples at (-) side moving seawards
					110	17			0187REF	15	0,175	0,170	Ripple at (-) moving seawards; ripple at (+) standing; small scour at (+)
					105	17				15	0,145	0,150	Movement of ripples as before; small scour at (+)
					95	13				15	0,155	0,155	Small scour at (+); movement of ripples as before
					110	16				15	0,165	0,155	Small scour at (+)
7	24,06	0,15	2,00	60	85	12	moderately	0,14	I_015_2	15	0,140	0,118	
(J)					90	15	regular		0197LOG1	15	0,100	0,070	
					95	15			0197REF	15	0,080	0,070	
					90	14	symmetric			15	0,075	0,085	
					95	13				15	0,080	0,090	
					100	12				15	0,075	0,085	

Table 4a continued.

Record of bedload measurements 1996 — Irregular waves: JONSWAP (J) & Pierson-Moskowitz (P-M) spectra

Water depth h=0.5 m

A two-cell sand trap; (+) and (-) denote the *onshore* and *offshore* directed sediment accumulated in the trap, respectively

Table shows significant wave height and peak period at the wave maker

Test No.	Date	H [m]	T [s]	Time after which the ripples were measured [min]	Ripple length [mm]	Ripple height [mm]	Ripple shape	Refl. coeff.	Data files	Accum. time [min]	Offshore directed accum. (-) [kg]	Onshore directed accum. (+) [kg]	Remarks
8	25,06	0,20	1,75	60	95	16	regular	0,13	I_02_175	15	0,250	0,205	Ripple crest effect at (-)
(J)					100	16	symmetric		0209LOG1	15	0,155	0,140	
					90	15			0209REF	15	0,140	0,140	
					85	14				15	0,130	0,125	
					85	13				15	0,110	0,110	
										15	0,115	0,117	
										15	0,100	0,100	
9	26,06	0,20	1,75	60	95	14	regular	0,14	I1_02_17	15	0,185	0,195	
(P-M)					80	12	symmetric		0221LOG1	15	0,122	0,152	
					80	12			0221REF	15	0,117	0,158	
					80	12				15	0,108	0,150	
					85	14				15	0,106	0,141	
					85	13				15	0,115	0,130	Small scour at (-)
										15	0,075	0,125	Small scour at (-)
10	27,06	0,15	2,00	60	80	12	regular	0,16	I1_015_2	15	0,125	0,105	
(P-M)					85	13	symmetric		0233LOG1	15	0,092	0,077	
					80	13			0233REF	15	0,082	0,074	
										15	0,069	0,083	
										15	0,064	0,080	
										15	0,057	0,067	

Table 5.

Bedload tests IBW 1996: irregular wave parameters at the sand trap												
Water depth h=0.5 m, registration ~ 15 min.												
Test No.	Spectrum	T_p [s]	H_rms [m]	Theta_2.5_rms	H_max [m]	k_s [m]	T_r [s]	q_b_sum measured [m3/m]	q_b_sum computed [m3/m]	% diff. meas./comp.	PhibT2 meas.	PhibT2 comp.
5	J	2.00	0.120	0.1318	0.285	0.0234	2.00	0.000952	0.000879	8	0.080531	0.074398
6	P-M	2.00	0.119	0.1300	0.278	0.0236	1.97	0.000863	0.000797	8	0.073008	0.067454
7	J	2.00	0.091	0.0848	0.229	0.0303	1.95	0.000432	0.000488	-12	0.036521	0.041302
8	J	1.75	0.117	0.1204	0.261	0.0246	1.80	0.000671	0.000753	-11	0.056775	0.063730
9	P-M	1.75	0.116	0.1188	0.272	0.0249	1.78	0.000651	0.000694	-6	0.055075	0.058736
10	P-M	2.00	0.092	0.0863	0.240	0.0299	1.92	0.000394	0.000468	-16	0.033341	0.039609